

# Macular Choroidal Thickness in Normal Pediatric Population Measured by Swept-Source Optical Coherence Tomography

José M. Ruiz-Moreno,<sup>1,2</sup> Iñaki Flores-Moreno,<sup>1</sup> Francisco Lugo,<sup>2</sup> Jorge Ruiz-Medrano,<sup>2</sup> Javier A. Montero,<sup>3</sup> and Masabiro Akiba<sup>4</sup>

**PURPOSE.** To evaluate choroidal thickness in healthy pediatric population by swept-source longer-wavelength optical coherence tomography (SS-OCT).

**METHODS.** This was a cross-sectional comparative, noninterventional study. The macular area of 83 eyes from 43 pediatric patients (<18 years) was studied with an SS-OCT prototype system. Macular choroidal thickness was manually determined at 750- $\mu$ m intervals by measuring the perpendicular distance from the posterior edge of the RPE to the choroid/sclera junction, along a horizontal 4500- $\mu$ m line centered in the fovea. Three observers independently determined choroidal thickness. Pediatric choroidal thickness was compared with choroidal thickness from 75 eyes from 50 normal healthy adult volunteers (18 years or older).

**RESULTS.** Mean age was  $10 \pm 3$  years (3–17) in the pediatric population versus  $53 \pm 16$  (25–85) in the adult population ( $P < 0.001$ ). Mean spherical equivalent was not different ( $P = 0.06$ ) between both groups. Mean subfoveal choroidal thickness was  $312.9 \pm 65.3$   $\mu$ m in the pediatric versus  $305.6 \pm 102.6$   $\mu$ m in the adult population ( $P = 0.19$ ). Mean macular choroidal thickness was  $285.2 \pm 56.7$   $\mu$ m in the pediatric versus  $275.2 \pm 92.7$   $\mu$ m in the adult population ( $P = 0.08$ ). The distribution of choroidal thickness along the horizontal line was different for both populations; the temporal choroid was thicker in the pediatric population (320, 322, and 324  $\mu$ m;  $P = 0.002$ , 0.001, and 0.06, respectively), followed by the subfoveal (312  $\mu$ m) and nasal choroid (281, 239, and 195  $\mu$ m).

**CONCLUSIONS.** Macular choroidal thickness in the pediatric population is not significantly thicker than that of healthy adults. Differences are more remarkable in the temporal side of the fovea. (*Invest Ophthalmol Vis Sci.* 2013;54:353–359) DOI: 10.1167/iovs.12-10863

From the <sup>1</sup>Department of Ophthalmology, Castilla La Mancha University, Albacete, Spain; the <sup>2</sup>Alicante Institute of Ophthalmology, VISSUM, Vitreo-Retinal Unit, Alicante, Spain; the <sup>3</sup>Pío del Río Horta University Hospital, Ophthalmology Unit, Valladolid, Spain; and the <sup>4</sup>Topcon Corporation, Tokyo, Japan.

Supported in part by a grant of the Spanish Ministry of Health, Instituto de Salud Carlos III, Red Temática de Investigación Cooperativa en Salud "Patología ocular del envejecimiento, calidad visual y calidad de vida" (RD07/0062/0019).

Submitted for publication August 29, 2012; revised November 5 and December 9, 2012; accepted December 9, 2012.

Disclosure: **J.M. Ruiz-Moreno**, None; **I. Flores-Moreno**, None; **F. Lugo**, None; **J. Ruiz-Medrano**, None; **J.A. Montero**, None; **M. Akiba**, TOPCON (E)

Corresponding author: Jose M. Ruiz-Moreno, Departamento de Ciencias Médicas, Facultad de Medicina, Avda. de Almansa, 14. 02006. Albacete, Spain; josemaria.ruiz@uclm.es.

**T**echnological advances and new information about the role of the choroid in ophthalmic pathology have promoted new research on choroidal anatomy and physiology.<sup>1</sup>

Choroidal changes are associated with some conditions such as central serous chorioretinopathy,<sup>2–5</sup> age-related macular degeneration,<sup>4–11</sup> polypoidal choroidal vasculopathy,<sup>4–7,10</sup> myopic maculopathy,<sup>12–16</sup> posterior uveitis,<sup>4,5,17–21</sup> and choroidal tumors.<sup>4,22,23</sup> Even though indocyanine green angiography (ICGA) and optical coherence tomography (OCT) have aided in the study of the choroid, adequate morphologic examination using spectral domain OCT (SD-OCT) has not been possible until recently due to the presence of pigment cells that attenuate the incident light, and the limited depth of penetration inherent to the design of SD-OCT instruments.<sup>1</sup>

It has been previously reported that choroidal thickness (as determined by SD-OCT) decreases with age in healthy eyes.<sup>24–29</sup> However, pediatric choroidal thickness has not been previously determined.

High penetration, swept-source longer-wavelength OCT (SS-OCT) has an innovative 1- $\mu$ m band light source,<sup>30–33</sup> longer than that of conventional machines, that provides higher penetration through the RPE, enabling deep choroidal imaging. There are no commercially available SS-OCT machines and prototypes are mainly used for research.

The aim of this study is to determine choroidal thickness in the pediatric population using a prototype SS-OCT.

## PATIENTS AND METHODS

A cross-sectional comparative, noninterventional study was performed at VISSUM Alicante, Spain. All examinations were obtained in the afternoon to avoid diurnal variations.<sup>34,35</sup> The institutional review board of VISSUM Alicante approved the use of the prototype SS-OCT and data collection. This study followed the tenets of the Declaration of Helsinki.

The macular area of a healthy pediatric population (<18 years) was studied with an SS-OCT prototype system (Topcon Corporation, Tokyo, Japan), after their parents provided informed consent. The SS-OCT prototype used to image the full-thickness choroid and sclera is based on SS-OCT technology,<sup>36</sup> which uses a tunable laser as a light source operated at a 100,000-Hz A-scan repetition rate in the 1- $\mu$ m wavelength region. The reference mirror is placed at the deepest position of the retina to increase sensitivity at the choroidal level in macular imaging. An OCT image contains 1024 axial scans and up to 96 images are considered for image averaging. Lateral resolution is 20  $\mu$ m while axial resolution is 8  $\mu$ m in the retina.<sup>37</sup> Lateral and axial resolution are independent.

Acquisition time was 1 second. Choroidal thickness was manually calculated as the perpendicular distance from the external surface of the RPE (hyperreflective line) to the internal surface of the sclera.

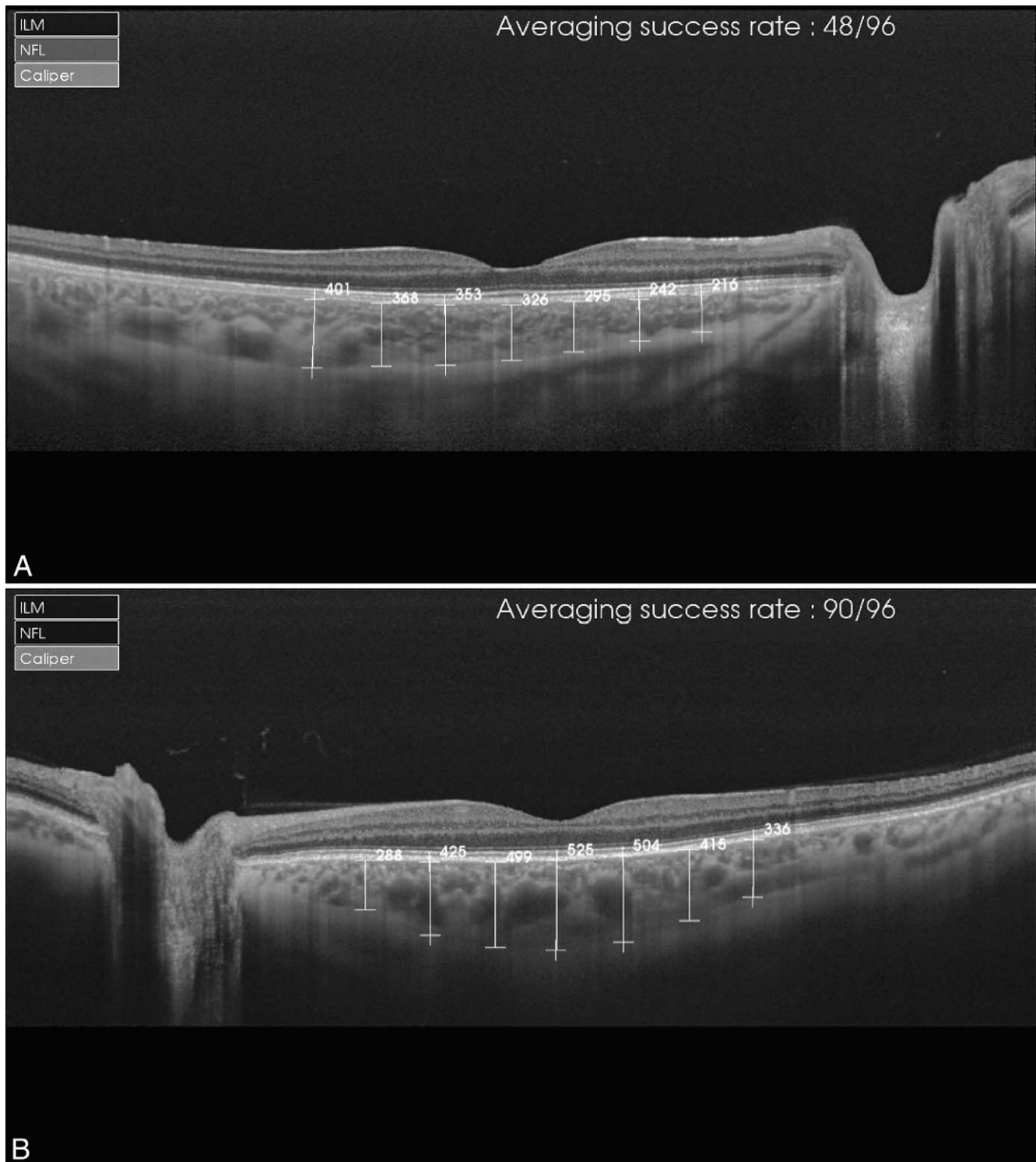


**FIGURE 1.** Choroidal thickness determinations (in  $\mu\text{m}$ ). **(A)** Pediatric eyes. **(B)** Adult eyes.

Choroidal thickness was determined under the fovea (subfoveal choroidal thickness); three further determinations were performed every 750  $\mu\text{m}$  temporal (T1, T2, and T3) and nasal (N1, N2, and N3) to the fovea (Fig. 1). Average macular horizontal choroidal thickness was calculated as the average of these seven determinations.

An average macular profile was calculated as a line formed by the mean values of each point (T3, T2, T1, subfoveal, N1, N2, and N3) in the pediatric and adult groups.

Pediatric choroidal thickness was compared with that of normal healthy adult volunteers (18 years or older). Eyes with spherical equivalent (SE) beyond  $\pm 6$  diopters (D) or ocular conditions were excluded from both groups. An experienced technician determined refractive errors using an auto-refractometer (Nidek, Gamagohri, Japan) that was later checked by a certified optometrist.

Three observers determined choroidal thickness independently and the final thickness was calculated as the arithmetic mean of the

calculations of the three observers. The interobserver reproducibility was evaluated using intraclass correlation coefficient and Bland Altman plots. Pearson's correlation was calculated for choroidal thickness and age and SE;  $P$  value  $< 0.05$  was considered statistically significant. Statistical analysis was performed using licensed statistical software (SPSS version 14.0; SPSS Inc., Chicago, IL).

## RESULTS

The macular area of 83 eyes from 43 healthy pediatric individuals ( $< 18$  years) was studied with an SS-OCT prototype system and compared with 75 eyes from 50 normal healthy adult volunteers (18 years or older).

SS-OCT allowed visualization of choroidal thickness in all the cases (100%) in both groups (Fig. 1). Mean age in the pediatric population was  $10 \pm 3$  years (3–17) versus  $53 \pm 16$  years (25–85) in the adult group ( $P < 0.001$ ; Student's  $t$ -test). Mean SE was similar in both groups ( $0.3 \pm 2.0$  D, range +3.75 to  $-5.25$  in children versus  $0.16 \pm 1.4$  D, range +3.25 to  $-5.0$  in adults;  $P = 0.06$ ; Student's  $t$ -test). Mean subfoveal choroidal thickness was  $312.9 \pm 65.3$   $\mu\text{m}$  (158–469) in children versus  $305.6 \pm 102.6$   $\mu\text{m}$  (152–624) in adults ( $P = 0.19$ ; Mann-Whitney  $U$  test). Average macular horizontal choroidal thickness was  $285.2 \pm 56.7$   $\mu\text{m}$  (153–399) in children versus  $275.2 \pm 92.7$   $\mu\text{m}$  (132–551) in adults ( $P = 0.08$ ; Mann-Whitney  $U$  test; Table 1).

Pediatric choroidal thickness was highest in the temporal side (320, 322, and 324  $\mu\text{m}$  for T3, T2, and T1, respectively; confidence intervals 13.2, 12.9, and 13.0  $\mu\text{m}$ , respectively); then in the fovea (312  $\mu\text{m}$ ; confidence interval 14.1  $\mu\text{m}$ ); and thinnest in the nasal side (281, 239, and 195  $\mu\text{m}$  for N1, N2, and N3 respectively; confidence intervals 14.1, 13.3, and 12.5  $\mu\text{m}$ , respectively). Adult choroidal thickness was highest in the fovea (305  $\mu\text{m}$ ; confidence interval 23.3  $\mu\text{m}$ ); followed by the temporal (281, 290, 299  $\mu\text{m}$  for T3, T2, and T1, respectively; confidence intervals 18.5, 20.3, and 21.6  $\mu\text{m}$ , respectively); and the nasal side (290, 253, 205  $\mu\text{m}$  for N1, N2, and N3 respectively; confidence intervals 23.8, 23.4, and 22.5  $\mu\text{m}$ , respectively; Fig. 2). Differences in choroidal thickness between both groups were statistically significant at T3 and T2 ( $P = 0.002$  and  $P = 0.01$ , respectively, Student's  $t$ -test) and near significance in T1 ( $P = 0.06$ , Student's  $t$ -test). Differences in subfoveal and nasal choroidal thickness were not statistically significant.

The average temporal choroidal thickness within the pediatric group was lower in the group formed by children 10 to 17 years ( $n = 35$  eyes) than among children aged 3 to 9 years ( $n = 48$  eyes); but the differences between both groups were less marked in the nasal sectors (Fig. 2B).

Correlation between macular horizontal choroidal thickness and age or SE and between subfoveal choroidal thickness and SE in the pediatric group was  $r = -0.25$  ( $P = 0.02$ );  $r = 0.37$  ( $P = 0.001$ ); and  $r = 0.41$  ( $P = 0.000$ ), respectively. Correlation between choroidal thickness and age in the whole population was weak or not significant at N3, N2, N1, and fovea, and significant at T1 ( $r = -0.22$ ,  $P = 0.004$ ); T2 ( $r = -0.29$ ,  $P = 0.000$ ); and T3 ( $r = -0.33$ ,  $P = 0.000$ ; Fig. 3).

The intraclass correlation coefficient for choroidal thickness for the three independent observers was between 0.91 and 0.98. The Bland-Altman plots showed small differences and narrow limits of agreement for choroidal thickness for interobserver comparison, suggesting satisfactory agreement between the observers. Most of the data points were tightly clustered around the zero line of the difference between the two choroidal thickness determinations and 95% to 97.5% of the determinations fell within limits of agreement (Fig. 4).

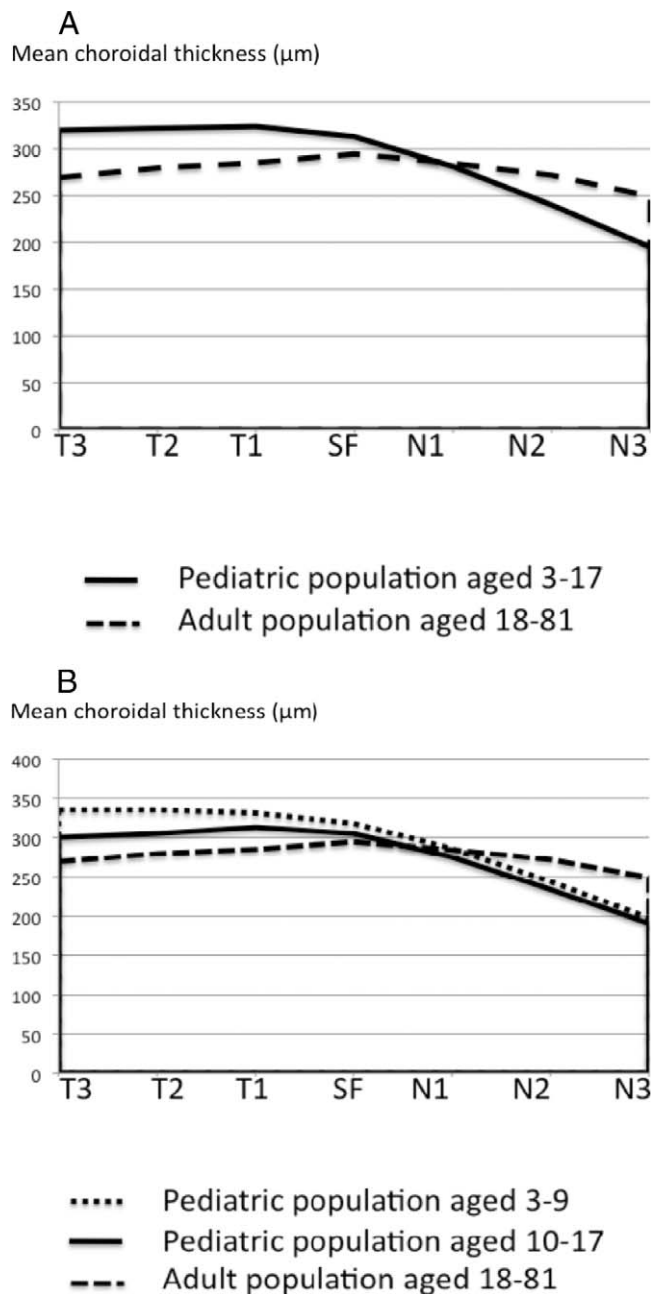


FIGURE 2. (A) Choroidal thickness profile in the pediatric versus the adult group. (B) The pediatric group has been split into two subgroups (aged 3–9 and 10–17 years) and the respective profiles are compared with the adult profile.

## DISCUSSION

Choroidal research has always been difficult. ICGA permits visualization of choroidal vessels<sup>4,5</sup> and recent advances in OCT technology have added cross-sectional information about the choroid.<sup>1</sup> Enhanced-depth imaging provided by SD-OCT has permitted cross-sectional research of the choroid, increasing our knowledge on the pathophysiology and etiology of several ocular conditions.<sup>2,3,6–23</sup> Long wavelength SS-OCT prototypes (1050–1060 nm) have been used in patients improving image quality. Faster and higher quality software may overcome RPE barrier effect and movement artifacts.<sup>11,26,38</sup>

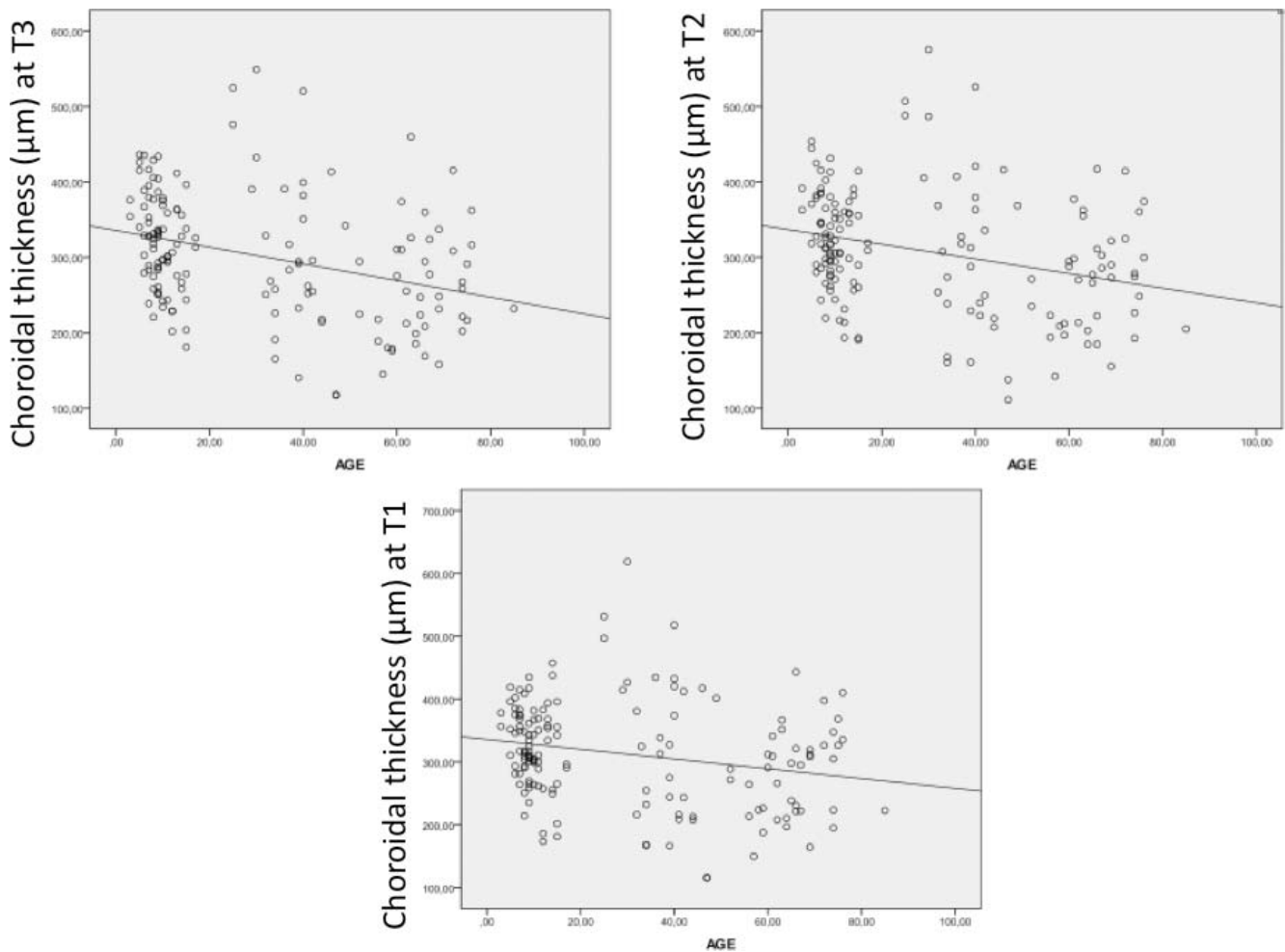


FIGURE 3. Scatterplot showing choroidal thickness at T3, T2, and T1 in the whole group. Choroidal thickness and age correlate significantly: T1 ( $r = -0.22, P = 0.004$ ); T2 ( $r = -0.29, P = 0.000$ ); and T3 ( $r = -0.33, P = 0.000$ ).

Papers on choroidal thickness report a progressive choroidal thinning associated with age.<sup>24–29</sup> Margolis described 1.56- $\mu\text{m}$  thinning for each year of life.<sup>28</sup> Agawa<sup>38</sup> and Li<sup>39</sup> reported that such correlation between choroidal thickness and age did not exist in eyes with axial length <25 mm. The effect of age on pediatric choroidal thickness has not been studied previously.

In our series, SS-OCT allowed visualization of the choroid in all the cases with high-quality images (Fig. 1), permitting choroidal thickness determination. Our data suggest that the temporal choroid may become thinner with age, even thinner

than the subfoveal choroid in the adult population. This finding is reinforced by the significant inverse correlation between choroidal thickness and age in the whole group at T1, T2, and T3 (Fig. 3).

The average values of choroidal thickness in our adult group were in agreement with previously reported series with similar age distribution (Table 2).<sup>25,27,28</sup> Due to the strong correlation between age and choroidal thickness in adults,<sup>28</sup> the age factor should be carefully considered when comparing populations with different age distributions.<sup>26,29,38,39</sup> Mean subfoveal choroidal thickness in our adult group ( $312.9 \pm 65.3 \mu\text{m}$ )

TABLE 1. Patients' Demographics and CT

	Pediatric Population	Adult Population	P Value
<i>n</i> (eyes)	83	75	
Mean age; y	9.6 $\pm$ 3.1; 3–17	53.2 $\pm$ 15.6; 25–85	$P < 0.001$ ; Student's <i>t</i> -test
Mean SE	0.3 $\pm$ 2.0 D; 3.75 to $-5.25$	$-0.16 \pm 1.4$ D; 3.25 to $-5.0$	$P = 0.06$ ; Student's <i>t</i> -test
Mean subfoveal CT	312.9 $\pm$ 65.3 $\mu\text{m}$ ; 158–469	305.6 $\pm$ 102.6 $\mu\text{m}$ ; 152–624	$P = 0.19$ ; Mann-Whitney <i>U</i> test
Mean macular CT	285.2 $\pm$ 56.7 $\mu\text{m}$ ; 153–399	275.2 $\pm$ 92.7 $\mu\text{m}$ ; 132–551	$P = 0.08$ ; Mann-Whitney <i>U</i> test
Subfoveal CT 95% CI	298.7–327.3 $\mu\text{m}$	281.9–329.4 $\mu\text{m}$	
Macular CT 95% CI	272.9–297.8 $\mu\text{m}$	250.0–293.3 $\mu\text{m}$	
Definite choroid/sclera junction, %	100	100	

CT, choroidal thickness.

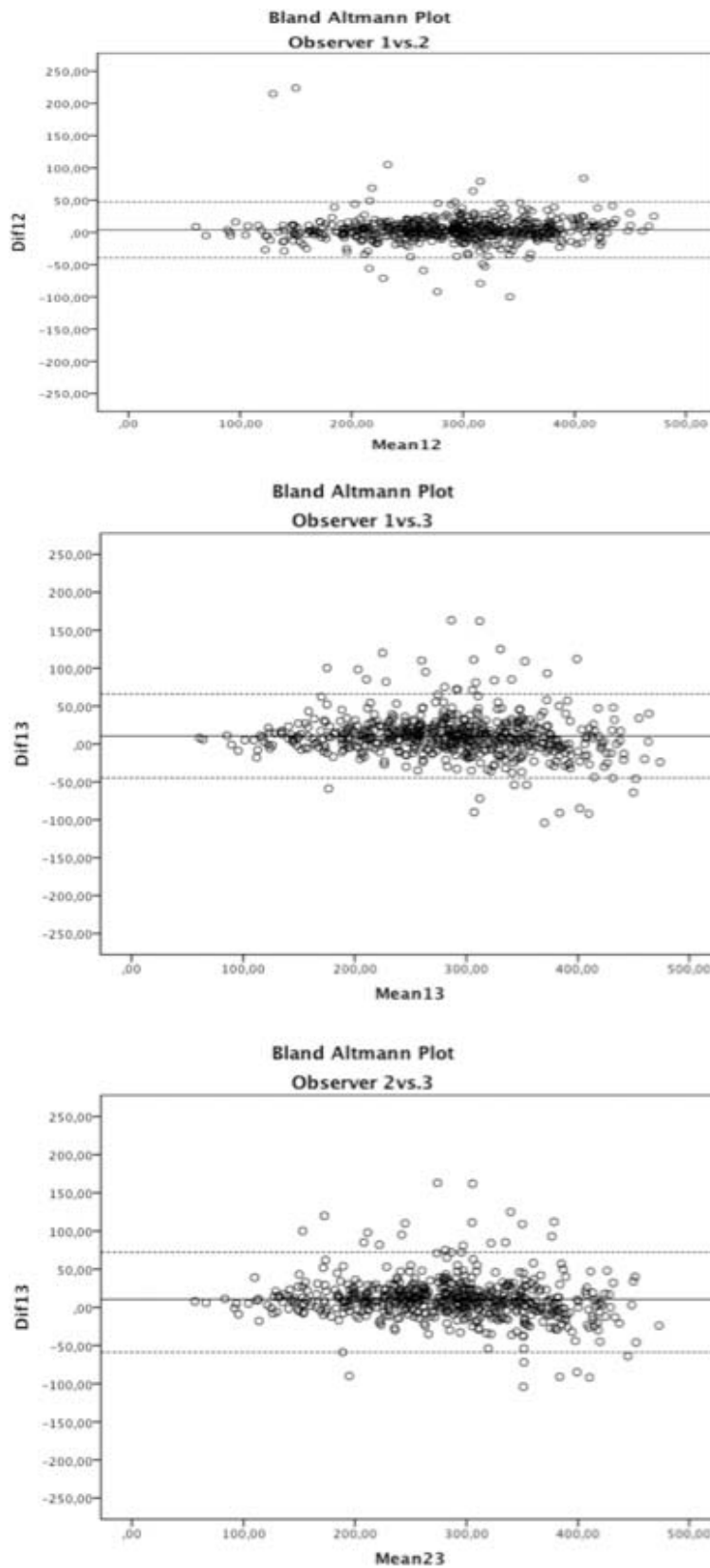


FIGURE 4. Bland-Altman plots representing the differences in interobserver determinations of choroidal thickness. *Solid lines* represent mean difference and *dashed lines* show the lower and upper 95% limits of agreement. Most of the data points are tightly clustered around the zero line of the difference between the two choroidal thickness determinations.

TABLE 2. Characteristics of Subfoveal CT

Study	Mean Age	Cases	Subfoveal CT	OCT System	Relation Age/CT	Definite Choroid/Sclera Junction, %
Ruiz-Moreno adult group	53.2	75	305	SS-OCT	-	100
Margolis <sup>28</sup>	50.4	54	287	Spectralis	+	
Manjunath <sup>27</sup>	51.1	34	272	Cirrus	+	74
Ikuno <sup>26</sup>	39.4	86	354	SS-OCT	+	
Agawa <sup>38</sup>	32.9	43	348	SS-OCT	-	
Li <sup>39</sup>	24.9	93	342			
Branchini <sup>1</sup>	35.2	28	337 to 347	Cirrus Spectralis RTVue		96.4
Ouyang <sup>29</sup>	32.8	59	297	Cirrus	-	100
Ruiz-Moreno pediatric population	9.6	83	312	SS-OCT	-/+	100

was higher than the average values reported in other series with younger patients (Table 2).

Even though the retinal landmarks may be slightly different from those reported in the literature, most of the choroidal thickness results were very similar considering Margolis' age-correction for choroidal thickness (1.56  $\mu\text{m}$  reduction per year).<sup>28</sup> We were unable to compare these data with those from our pediatric group since such data have not been previously reported. In our series, we have not found significant differences between adults and children except for the temporal choroid. The age at which subfoveal choroidal thickness starts to decrease, as has been suggested by some authors, is still to be determined.<sup>28</sup> This decline is probably related to aging vascular changes. We have found a significant correlation between macular choroidal thickness and age, macular choroidal thickness, and SE and between subfoveal choroidal thickness and SE within the pediatric group.

The topographic profile of choroidal thickness in the adult group in our series (Fig. 2) was highest in the subfoveal area, followed by the temporal and the nasal areas, as has been previously reported in other series.<sup>1,26-29</sup> However, this profile was different in the pediatric population: choroidal thickness was highest in the temporal choroid with 320, 322, and 324  $\mu\text{m}$ , followed by the subfoveal choroid with 312  $\mu\text{m}$  and the nasal choroid with 281, 239, and 195  $\mu\text{m}$ ; Fig. 2).

The subgroup analyses of the pediatric population showed that the profile of choroidal thickness seems to change progressively during the second decade of life, as the child grows older. These changes in choroidal thickness probably reflect vascular remodeling associated with choroidal maturation. The higher metabolic needs of the fovea compared with the surrounding retina may cause a reduction of the thickness of the temporal choroid, while sparing the subfoveal choroid.

OCT devices reported in the literature provide different qualities of imaging, permitting a more or less adequate visualization of the line delimiting the choroid and the sclera. In our series, all the patients examined by SS-OCT showed a clearly defined, measurable posterior portion of the choroid. Measurable choroidal thickness has been reported in 74%<sup>27</sup> to 90%<sup>25</sup> of the eyes examined by Cirrus HD-OCT and in 95.8% of the eyes examined by Heidelberg EDI-OCT.<sup>40</sup> Two papers comparing OCT equipments reported 96.4%<sup>1</sup> and 90.7% measurability.<sup>41</sup> Choroidal visualization was better in those studies using longer wavelength equipments. The high intra-class correlation coefficient (0.91-0.98) and the narrow limits of agreement of the Bland-Altman plots for the three independent observers highlight SS-OCT accuracy in choroidal thickness determination.

In the present study, we have considered SE instead of axial length determinations since previous indications from the literature show that refraction, which is more convenient to

obtain, provides equivalent modeling capability as axial length.<sup>42</sup>

Among the limitations of this study, we may mention that choroidal thickness has to be manually determined since there is no commercially available automated software. To our best knowledge, this is the first report of choroidal thickness determination in children using SS-OCT. A few studies have been previously performed in adults using SS-OCT<sup>26,36,38</sup> with different age distributions.

According to our results, macular choroidal thickness is similar in the healthy pediatric and adult population with different choroidal thickness profiles. New studies about choroidal thickness in pediatric population are required to confirm our findings. Knowledge of the normal choroidal thickness and choroidal thickness profile may aid in the understanding of normal changes and the appearance of chorioretinal conditions in pediatric eyes.

## References

- Branchini L, Regatieri CV, Flores-Moreno I, Baumann B, Fujimoto JG, Duker JS. Reproducibility of choroidal thickness measurements across three spectral domain optical coherence tomography systems. *Ophthalmology*. 2012;119:119-123.
- Imamura Y, Fujiwara T, Margolis R, Spaide RE. Enhanced depth imaging optical coherence tomography of the choroid in central serous chorioretinopathy. *Retina*. 2009;29:1469-1473.
- Maruko I, Iida T, Sugano Y, Ojima A, Sekiryu T. Subfoveal choroidal thickness in fellow eyes of patients with central serous chorioretinopathy. *Retina*. 2011;31:1603-1608.
- Stanga PE, Lim JJ, Hamilton P. Indocyanine green angiography in chorioretinal diseases: indications and interpretation: an evidence-based update. *Ophthalmology*. 2003;110:15-21. quiz 22-23.
- Yannuzzi LA. Indocyanine green angiography: a perspective on use in the clinical setting. *Am J Ophthalmol*. 2011;151:745-751.e1.
- Chung SE, Kang SW, Lee JH, Kim YT. Choroidal thickness in polypoidal choroidal vasculopathy and exudative age-related macular degeneration. *Ophthalmology*. 2011;118:840-845.
- Koizumi H, Yamagishi T, Yamazaki T, Kawasaki R, Kinoshita S. Subfoveal choroidal thickness in typical age-related macular degeneration and polypoidal choroidal vasculopathy. *Graefes Arch Clin Exp Ophthalmol*. 2011;249:1123-1128.
- Manjunath V, Goren J, Fujimoto JG, Duker JS. Analysis of choroidal thickness in age-related macular degeneration using spectral-domain optical coherence tomography. *Am J Ophthalmol*. 2011;152:663-668.
- Switzer DW Jr, Mendonca LS, Saito M, Zweifel SA, Spaide RE. Segregation of ophthalmoscopic characteristics according to choroidal thickness in patients with early age-related macular degeneration. *Retina*. 2012;32:1265-1271.

10. Ueta T, Obata R, Inoue Y, et al. Background comparison of typical age-related macular degeneration and polypoidal choroidal vasculopathy in Japanese patients. *Ophthalmology*. 2009;116:2400-2406.
11. Wood A, Binns A, Margrain T, et al. Retinal and choroidal thickness in early age-related macular degeneration. *Am J Ophthalmol*. 2011;152:1030-1038.e2.
12. Chen W, Wang Z, Zhou X, Li B, Zhang H. Choroidal and photoreceptor layer thickness in myopic population. *Eur J Ophthalmol*. 2012;22:590-597.
13. Fujiwara T, Imamura Y, Margolis R, Slakter JS, Spaide RF. Enhanced depth imaging optical coherence tomography of the choroid in highly myopic eyes. *Am J Ophthalmol*. 2009;148:445-450.
14. Fureder W, Krauth MT, Sperr WR, et al. Evaluation of angiogenesis and vascular endothelial growth factor expression in the bone marrow of patients with aplastic anemia. *Am J Pathol*. 2006;168:123-130.
15. Ikuno Y, Tano Y. Retinal and choroidal biometry in highly myopic eyes with spectral-domain optical coherence tomography. *Invest Ophthalmol Vis Sci*. 2009;50:3876-3880.
16. Wang NK, Lai CC, Chu HY, et al. Classification of early dry-type myopic maculopathy with macular choroidal thickness. *Am J Ophthalmol*. 2012;153:669-677.e2.
17. Aoyagi R, Hayashi T, Masai A, et al. Subfoveal choroidal thickness in multiple evanescent white dot syndrome. *Clin Exp Optom*. 2012;95:212-217.
18. Channa R, Ibrahim M, Sepah Y, et al. Characterization of macular lesions in punctate inner choroidopathy with spectral domain optical coherence tomography. *J Ophthalmic Inflamm Infect*. 2012;2:113-120.
19. Fong AH, Li KK, Wong D. Choroidal evaluation using enhanced depth imaging spectral-domain optical coherence tomography in Vogt-Koyanagi-Harada disease. *Retina*. 2011;31:502-509.
20. Maruko I, Iida T, Sugano Y, et al. Subfoveal choroidal thickness after treatment of Vogt-Koyanagi-Harada disease. *Retina*. 2011;31:510-517.
21. Nakai K, Gomi F, Ikuno Y, et al. Choroidal observations in Vogt-Koyanagi-Harada disease using high-penetration optical coherence tomography. *Graefes Arch Clin Exp Ophthalmol*. 2012;250:1089-1095.
22. Say EA, Shah SU, Ferenczy S, Shields CL. Optical coherence tomography of retinal and choroidal tumors. *J Ophthalmol*. 2011;2011:385058.
23. Shields CL, Perez B, Materin MA, Mehta S, Shields JA. Optical coherence tomography of choroidal osteoma in 22 cases: evidence for photoreceptor atrophy over the decalcified portion of the tumor. *Ophthalmology*. 2007;114:e53-e58.
24. Ding X, Li J, Zeng J, et al. Choroidal thickness in healthy Chinese subjects. *Invest Ophthalmol Vis Sci*. 2011;52:9555-9560.
25. Ho J, Branchini L, Regatieri C, Krishnan C, Fujimoto JG, Duker JS. Analysis of normal peripapillary choroidal thickness via spectral domain optical coherence tomography. *Ophthalmology*. 2011;118:2001-2007.
26. Ikuno Y, Kawaguchi K, Nouchi T, Yasuno Y. Choroidal thickness in healthy Japanese subjects. *Invest Ophthalmol Vis Sci*. 2010;51:2173-2176.
27. Manjunath V, Taha M, Fujimoto JG, Duker JS. Choroidal thickness in normal eyes measured using Cirrus HD optical coherence tomography. *Am J Ophthalmol*. 2010;150:325-329.e1.
28. Margolis R, Spaide RF. A pilot study of enhanced depth imaging optical coherence tomography of the choroid in normal eyes. *Am J Ophthalmol*. 2009;147:811-815.
29. Ouyang Y, Heussen FM, Mokwa N, et al. Spatial distribution of posterior pole choroidal thickness by spectral domain optical coherence tomography. *Invest Ophthalmol Vis Sci*. 2011;52:7019-7026.
30. Huber R, Adler DC, Srinivasan VJ, Fujimoto JG. Fourier domain mode locking at 1050 nm for ultra-high-speed optical coherence tomography of the human retina at 236,000 axial scans per second. *Opt Lett*. 2007;32:2049-2051.
31. Lim H, de Boer JF, Park BH, Lee EC, Yelin R, Yun SH. Optical frequency domain imaging with a rapidly swept laser in the 815-870 nm range. *Opt Express*. 2006;14:5937-5944.
32. Unterhuber A, Povazay B, Hermann B, Sattmann H, Chavez-Pirson A, Drexler W. In vivo retinal optical coherence tomography at 1040 nm - enhanced penetration into the choroid. *Opt Express*. 2005;13:3252-3258.
33. Yasuno Y, Hong Y, Makita S, et al. In vivo high-contrast imaging of deep posterior eye by 1-micron swept source optical coherence tomography and scattering optical coherence angiography. *Opt Express*. 2007;15:6121-6139.
34. Brown JS, Flitcroft DI, Ying GS, et al. In vivo human choroidal thickness measurements: evidence for diurnal fluctuations. *Invest Ophthalmol Vis Sci*. 2009;50:5-12.
35. Tan CS, Ouyang Y, Ruiz H, Sadda SR. Diurnal variation of choroidal thickness in normal, healthy subjects measured by spectral domain optical coherence tomography. *Invest Ophthalmol Vis Sci*. 2012;53:261-266.
36. Ikuno Y, Maruko I, Yasuno Y, et al. Reproducibility of retinal and choroidal thickness measurements in enhanced depth imaging and high-penetration optical coherence tomography. *Invest Ophthalmol Vis Sci*. 2011;52:5536-5540.
37. Hirata M, Tsujikawa A, Matsumoto A, et al. Macular choroidal thickness and volume in normal subjects measured by swept-source optical coherence tomography. *Invest Ophthalmol Vis Sci*. 2011;52:4971-4978.
38. Agawa T, Miura M, Ikuno Y, et al. Choroidal thickness measurement in healthy Japanese subjects by three-dimensional high-penetration optical coherence tomography. *Graefes Arch Clin Exp Ophthalmol*. 2011;249:1485-1492.
39. Li XQ, Larsen M, Munch IC. Subfoveal choroidal thickness in relation to sex and axial length in 93 Danish university students. *Invest Ophthalmol Vis Sci*. 2011;52:8438-8441.
40. Mwanza JC, Hochberg JT, Banitt MR, Feuer WJ, Budenz DL. Lack of association between glaucoma and macular choroidal thickness measured with enhanced depth-imaging optical coherence tomography. *Invest Ophthalmol Vis Sci*. 2011;52:3430-3435.
41. Yamashita T, Shirasawa M, Arimura N, Terasaki H, Sakamoto T. Repeatability and reproducibility of subfoveal choroidal thickness in normal eyes of Japanese using different SD-OCT devices. *Invest Ophthalmol Vis Sci*. 2012;53:1102-1107.
42. Nishida Y, Fujiwara T, Imamura Y, Lima LH, Kurosaka D, Spaide RF. Choroidal thickness and visual acuity in highly myopic eyes. *Retina*. 2012;32:1229-1236.